Benchmarking Study of Demolition Wastes with Different Waste Materials as Sensible Thermal Energy Storage

B. Kocak[a,b,c], A.I. Fernandez[c], H. Paksoy[a*]

[a] *Cukurova University, Department of Chemistry, Faculty of Art and Science, Adana, Turkey,*

[b]*Çukurova University, Central Research Laboratory (CUMERLAB), Adana, Turkey*

[c]*DIOPMA Centre, Department of Materials Science & Physical Chemistry, Universitat de Barcelona, Martí i Franquès, 1, 08028, Barcelona, Spain*

(kocakburcu@gmail.com, ana_inesfernandez@ub.edu, hopaksoy@cu.edu.tr)

**Halime Paksoy, Balcali Mah. Saricam, 01310 Adana Turkey, Tel: +90 322 338 6084, Fax: +90 322 338 6945, hopaksoy@cu.edu.tr*

Abstract

Waste materials have a great potential as sustainable and cheap sensible thermal energy storage material (STESM). There are a number of previous studies on the use of wastes as STESM such as Cofalit, coal fly ash and electric arc furnace slags, by-products of the ilmenite mining industry and by-products of the potash production, municipal waste glass and by-products generated in steel industry. The aim of this study is to assess demolition wastes (DW) from urban regenerations in Turkey as a STESM and compare relevant properties with other waste and by-product storage materials. Results show that DW developed here has better or similar storage performance compared to other STESM from wastes. DW is found to be durable up to 750 ºC and can be used for high temperature thermal energy storage applications in packed beds.

Keywords: Thermal energy storage, Sensible thermal energy storage materials, demolition wastes, industrial by-products, waste materials

1. Introduction

Industrial development and rapid population growth increase total energy consumption in the world. Energy systems are generally based on the use of fossil fuels. In addition to increase in energy prices, use of fossil fuels affect the environment adversely by increasing CO_2 concentration in the atmosphere. Solar energy being the major renewable source is the main alternative to fossil fuels. Waste heat from industrial processes is also considered as a renewable energy resource to decrease fossil fuel-based energy consumption. Thermal energy storage (TES) systems are necessary to cover the mismatch between supply and demand of such fluctuating resources. Among the TES methods, sensible thermal energy storage (STES) systems can provide sustainable, cheap and eco-friendly energy to the users. More efficient and economical exploitation of alternative resources can be realized through integration of STES in the energy system. For industrial scale applications abundance, cost and durability of STES materials (STESM) are especially important.

Any solid material can be considered as STESM. Fernandez et al. [1] used CES selector software to determine which of these vast materials the best alternatives for sensible storage are. Based on this work, Khare et al. [2] gave the following expected properties for appropriate STESMs:

- Thermophysical properties: High energy density, heat capacity and conductivity and long-term thermal cycling stability.
- Chemical properties: Chemical stability, non-toxic, non-explosive, low potential reactivity with the heat transfer fluid (HTF) and the container material.
- Mechanical properties: Good mechanical stability, low coefficient of thermal expansion, high fracture toughness and high compressive strength.
- Economic properties: Cheap and abundant materials with low cost of manufacturing into suitable shapes.

Water is the cheapest medium with the highest energy density. On the other hand, water in liquid form can only be used for low temperature storage applications up to 100ºC. In literature there are a lot of studies on STESM from natural sources. Natural materials such as river rocks, gneiss rocks, desert sands, quartzite-rocks are good candidates for high temperature TES systems. Even if, these natural materials have high density up to 3200 kgm^{-3}, their specific heat capacities are limited between 700 – 1100 $Jkg^{-1}K^{-1}$ depending on rock structure [3-13]. Basalt is suggested as an alternative storage material with its stable, non-explosive and high energy density properties [11, 14-17].

Main advantages of using natural materials are: a) abundance and low-cost, b) suitability for high temperature applications, c) mechanical and thermal stability, d) no reaction with HTF in direct use [18]. Alumina is another alternative storage material, which can be used directly as aluminum beads or as composite material [2, 19, 20, 21]. Compared with rocks, alumina has higher thermal conductivity, this brings shorter charge and discharge time. On the other hand, high cost and low specific heat capacity make the system using alumina more expensive [22].

Molten salt commonly used for high temperature applications is the general name used for inorganic salts in their liquid phase. Among these, solar salt mixture (60% $NaNO_3$-40% KNO_3) is used in several commercial concentrated solar power plants (CSP). Operation temperature range for solar salt is limited between 220-565 ºC. It is relatively cheap, but it freezes below 220°C and is very corrosive. This may require expensive anti-freeze solutions and continuous heat supply. In addition, thermal conductivity values are too low, approximately 0.5 $Wm^{-1}K^{-1}$. The most mature storage technology is 2-tank storage system filled with molten salt. But the main drawback is the necessity of complex and expensive heat exchanger devices [23-25].

Thousand tons of storage material may be needed for especially industrial scale applications to store high amount of thermal energy. This increases investment cost and will affect the environment [26]. Researchers are now focusing on thermocline and packed-bed storage systems more, because single tank storage systems offer advantages by using low cost filler materials [27].

Waste materials have a great potential as STESM. Reducing and recycling of waste materials towards a circular economy is included in sustainability agenda of governments and industries. Advantage of using by-products and waste materials is to reduce the consumption of new/natural materials, to create low cost alternative storage materials and ultimately decrease use of fossil fuels [28]. Using inertized products derived from waste materials of different sources in STES is a sustainable way of valorization. These materials were first considered as fillers in direct molten salt storage applications. Motte et al. [29] investigated usability of wastes from different sources such as asbestos containing (Cofalit), coal fired power plants (CFA), electric arc furnaces (EAF) and blast furnaces (BFA) as fillers. As a result, Cofalit, CFA and BFA were recommended as alternative filler materials in direct solar molten salt systems. On the other hand, due to the high iron content, EAF was not suitable. Calvet et al

[30] filled thermocline tank with Cofalit in ceramic form, which was produced by applying high temperature plasma at 1500 °C to asbestos containing wastes. Cofalit in this form was stable up to 500 ºC in direct contact with nitrate salt and recommended as a low-cost filler material.

According to Naimi et al. [31], wastes from metal industries have a great potential with their low-cost, abundant, chemical and thermal stable properties. In addition to EAF slag, ladle furnace (LF) slag, aluminum pot skimming (APS) and aluminum white dross (AWD) can be used up to 1000°C in TES applications.

Navarro et al. [32] investigated by-products derived from the pyrometallurgical refining process of copper (Slag P), steelmaking process in electric arc furnace (WDF), the potash production process (IB) and ilmenite mining process (WrutF) as solid STESM. These materials were defined as low cost STESM with maximum unit cost of 0.15 €/kg.

Most of the wastes investigated as STESM are slags from different types of furnaces in metallurgical industry. Wang et al [33] presented thermal and microstructure properties of EAF slag samples from steelmaking industry to prove the feasibility as heat storage material. Grosu et al [34] evaluated a by-product from steel industry that is formed during the solidification of the steel in basic oxygen furnace (BOF). BOF slag was used as a filler material for a pre-industrial 20MWhth thermocline packed bed TES system with a storage efficiency of 76%. Fernandez et al. [35] investigated two other slags from electric arc furnace of steel making process. One (EAF Slag 1) was obtained by fast cooling with water, while the other one (EAF Slag 2) was produced by low slow cooling with open-air. Both materials were found to be stable up to 1100 ºC and have potential to be used in CSPs at temperatures above 600 ºC. Agalit et al. [36] investigated induction furnace slag (IFS) and recommended it as a candidate STESM up to 1000ºC with a volumetric heat capacity of 1850 $Jm^{-3}K^{-1}$.

Asbestos containing wastes (ACW) is another group that has been researched as potential STESMs. Py et al. [37] investigated cycled industrial ceramics made by vitrification of ACW. This material was suggested as a potential TES material up to 1200 ºC with high energy density and low cost. Faik et al. [38] analyzed ACW and fly ashes (FA) from municipal solid waste incineration to evaluate their thermal properties. Physical and chemical characteristics of ACF and FA proved that these inertized materials could be candidates for STESM.

Miro et al. [39] studied by-products from potash industry in STES system from 100ºC to 200ºC applications. Granulated by-product with 1-2 mm particle size was mainly composed of NaCl. By-product was analyzed both as directly in molten form (Salt A) and as solid form with low porosity after water treatment (Salt B). After water treatment, sample thermal conductivity and density increased. Cycling performance was determined as 63% for Salt A and 88% for Salt B.

Demolition waste (DW) is the most voluminous and substantial waste material. In Europe, over 800 million tons of waste is generated from partial or total demolition of residential, commercial and municipal buildings, roads or civil infrastructures [40]. According to EU Construction and Demolition Waste Management Protocol [41], demolition waste accounts for 33% of all wastes and it includes building components such as gypsum, plywood, chip wood, sawdust, brick, concrete, rock, metal, plastic and cardboard. Waste Framework Directive (2008/98/EC) [42] commits that minimum of 70% (by weight) of non-hazardous demolition wastes will be recycled by 2020. Therefore, valorization of DW is an important issue.

The aim of the present work is characterization of DW from urban regeneration projects in Turkey and comparison with other waste/by-product STESMs found in literature.

2. Materials and Method

DW used in this study was taken from an urban regeneration project in Adana, Turkey. Basic processes such as drying, crushing, sieving and mixing were applied to DW samples to develop homogeneous and durable STES material. A mortar was prepared with DW powders and CEM I 52.5 white Portland cement (WC). The best mortar formulation was determined as 0.90:0.10 (DW: WC) by mass in our previous study [28]. Paste mixture formed by adding water to the mortar was poured into cubic molds with dimensions of 0.5x0.5x0.5 mm^3 and spherical molds with 10 mm diameter. Uniform shaped STES samples were obtained after drying for 8 hours in oven at 150 °C.

Elemental analysis of DW dust was made using PANalytical, MiniPal 4XRay Fluorescence device. Further chemical analysis was done by Fourier-transform infrared spectroscopy with attenuated total reflection (FTIR ATR) under the wavelength from 450 to 4000 cm^{-1}, using Spectrum Two™ equipment from PerkinElmer. The test was done.

For thermal properties, Differential Scanning Calorimeter (Mettler Toledo, DSC 3+ Star System) was used to determine specific heat capacities (Cp) of DW samples. In DSC analysis, the samples were heated up to 400°C at a constant heating rate of 20°C/min. Thermal stabilities of DW samples were analyzed with thermogravimetric analyzer (Mettler Toledo, TGA/DSC 3+ Star System). Thermal conductivity measurements of DW samples both in powder and pellet forms were done by Hot Disk TPS 2500 S Thermal Conductivity Analyzer device.

Surface area and porosity of DW samples were evaluated by BET TriStar 3000 surface area and porosimeter measurement device under pure Nitrogen flow at -196 ˚C. Also, microscopic images of DW samples were taken using Zeiss Axiovert S100 microscope.

Density of DW dust was measured by AccuPyc 1330 V3.03 pycnometer. Helium gas displacement method was used to determine the volume of DW sample with this pycnometer.

Compressive strength tests done according to TS EN 12390-3 international standard were applied on 5x5x5 cm^3 of cubic DW samples using single axial load measurement device.

Structural, mechanical, chemical and thermal properties of waste materials to be compared with DW in this paper were obtained from the references indicated in Table 1. Although test methods in this study are similar with references, device, operator, environmental conditions can be different. Since the tests are carried out according to international standards, it is expected that comparing the test results of this study with another study in literature will not have a significant impact on benchmarking.

3. Results and Discussion

DW samples before and after development into STESM are shown in Figure 1. In order to assess potential of DW as STESM, the characterization results are compared with other waste/by-products found in literature.

(a) (b)

Figure 1. DW samples; (a) original form, (b) after moulding in spherical geometry with 10 mm diameter

3.1 Structural Properties

3.1.1 Material Forms and Preparation Methods

Waste materials developed as STESM in literature can be classified into three groups as asbestos containing wastes (ACW), industrial by-products and industrial wastes. Table 1 lists these waste materials together with DW developed here according to their origin, form and preparation methods. Depending on the origin of material, waste materials can be found in powder, slag or solid forms.

Table 1. Material forms and preparation methods of waste materials.

Group	Name	Origin	Form	Preparation Method	Ref
Construction and demolition wastes	**DW**	DW from urban regeneration projects	Solid particles	Crushing, sieving, mortar formulation, molding, drying	[28]
Asbestos containing wastes	**Ceramic Cofalit**	Asbestos containing waste	Solid particle	- Direct use of solids - Crushing, compressing	[26, 37]
	Glassy Cofalit (IACW)	Vitrification of asbestos containing wastes	Solid particle	- Directly manufactured with the desired shape	[26, 37]
Industrial by-products	**WrutF**	By-product from ilmenite mining process	Powder	Crushing then direct use of powder	[32]
	IB	By-product from potash production process	Powder	Crushing, sieving, compression	[32]
	WDF	By-product from steelmaking process in electric arc furnace	Powder	Crushing, sieving, compression	[32]
	Slag B / Slag P	By-products of the pyrometallurgical refining process of copper	Powder	Crushing, mortar formulation	[32]
	PP	By-products of the pyrometallurgical refining process of copper	Solid particle after molding	Mortar formulation of portland cement:Slag P (25:75)	[32]

	PB	By-products of the pyrometallurgical refining process of copper	Solid particle after molding	Mortar formulation of portland cement:Slag B (25:75)	[32]
	AP	By-products of the pyrometallurgical refining process of copper	Solid particle after molding	Mortar formulation of aluminious cement:Slag P (25:75)	[32]
	AB	By-products of the pyrometallurgical refining process of copper	Solid Particle after molding	Mortar formulation of aluminious cement:Slag B (25:75)	[32]
	CBPC_P	By-products of the pyrometallurgical refining process of copper	Solid Particle after molding	Mortar formulation of phospate cement:Slag P (20:75)	[32]
	CBPC_B	By-products of the pyrometallurgical refining process of copper	Solid Particle after molding	Mortar formulation of phospate cement:Slag B (20:75)	[32]
	BOF	By-product from steel industry	Slag	Direct use of slag	[27, 34]
	Salt A/B	By-product from potash industry	Granules	A: Direct use of granules B: Water treatment, molding, drying	[39]
Industrial wastes	**EAF**	Post-industrial product from electric arc furnaces	Slag	Crushing, compressing	[29]
	EAF Slag1	Electric arc furnace slag from steel making process	Slag	Direct use of slags	[35]
	EAF Slag2	Electric arc furnace slag from steel making process	Slag	Direct use of slags	[35]
	C EAF Slag	Electric arc furnace slag from steel making process	Slag	Direct use of slag	[33]
	S EAF Slag	Electric arc furnace slag from steel making process	Slag	Direct use of slag	[33]
	IFS	Induction furnace slag from steel making process	Slag	Direct use of slag	[36]
	BFA	Blast furnace slag from steel industry	Slag	Crushing, compressing	[29]
	CFA	Post-industrial product from coal fired power plants	Powder	Crushing, compressing	[29]
	Conv.	Converter steel slag	Slag	Crushing, compressing	[29]

Properties like humidity, dimension, shape, density and material composition can vary significantly for these waste materials given in Table 1. Therefore, some of these materials need to be subjected to pre-treatment processes such as crashing, sieving, drying, pressing, melting, molding, mixing, and compressing to prepare homogeneous STESM from waste materials [28].

ACWs, which are commercially known as Cofalit, were treated at high temperature (1500ºC) using plasma or microwave methods to convert them into a rock structure [26]. ACW can be available in ceramic or glass forms depending on thermal conditions of cooling treatment [26, 29, 30, 37]. Figure 2 shows the pictures of different ACWs. In Figure 2 a, b rock forms obtained from exit of the furnace with as-received shape are shown. ACW can also be obtained in molten form during the industrial process. This allows molding it in the desired shape without the need of extra melting process (Figure 2 c, d).

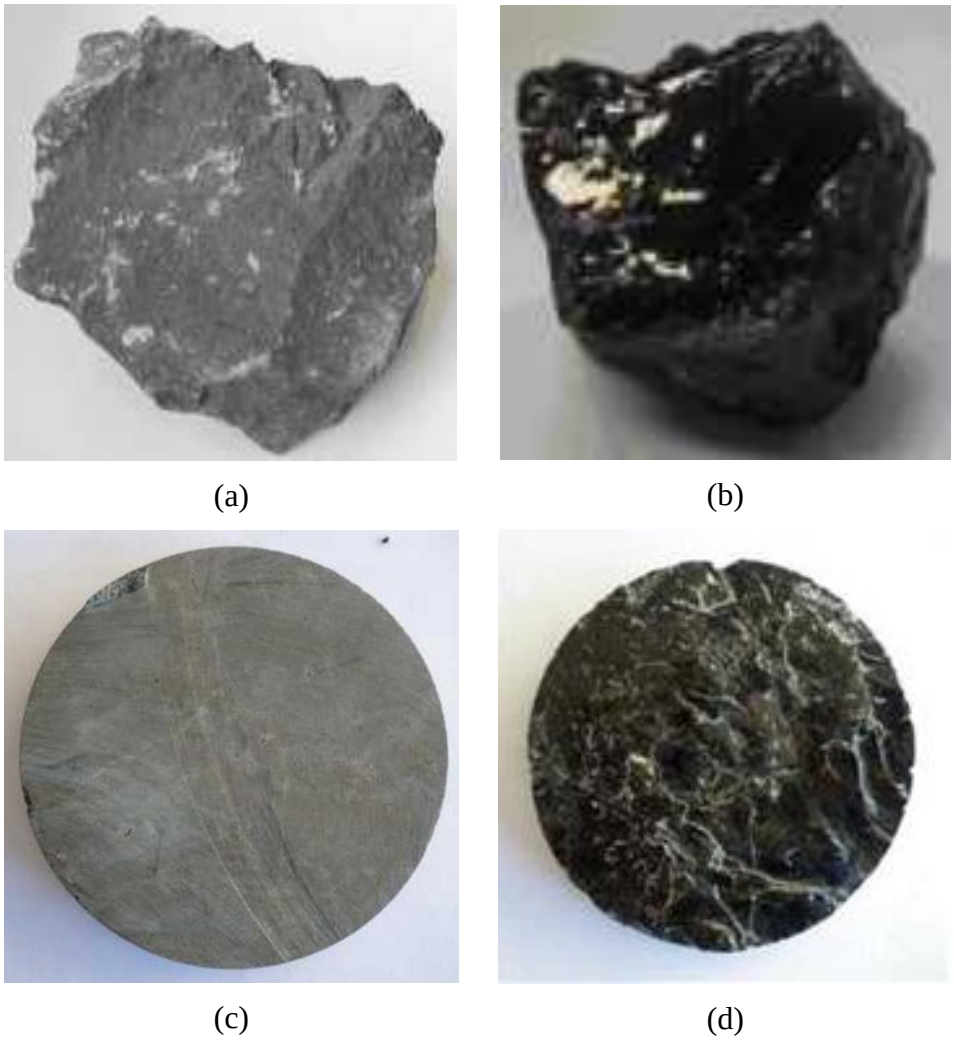

(a) (b)

(c) (d)

Figure 2. Asbestos containing wastes; a) As-received ceramic Cofalit [26], b) As-received glassy Cofalit [26], c) Desired shape ceramic Cofalit [37], d) Desired shape glassy Cofalit [37]

WrutF, IB, WDF, slag B, slag P, and CFA are received in powder form from their sources. Although these waste materials are in powder form, additional processes such as crushing, sieving and compressing were applied to produce samples with uniform particle size and desired shape. WrutF being in homogeneous powder form can be used directly or by compressing into desired shape [32]. IB and WDF were crushed to obtain homogeneous particles in 1 mm diameter range and then compressed for shape stabilization [32]. Compressing or molding processes could not be applied on Slag P and Slag B. STESM samples (PP, PB, AP, AB, CBPC_B, CBPC_P) from Slag P and Slag B were prepared by formulating mortars with CEM I 52,5R Portland, aluminous and phosphate cements [32]. Motte et al [29]

investigated coal fired power plant fly ash (CFA) wastes as STESM by compressing powder samples below 10 μm diameter.

Electric Arc Furnace slags (EAF, EAF Slag 1, EAF Slag 2, C EAF Slag, S EAF Slag) are waste materials from steel making processes in which ferrous steel scrap and fluxing agent (alumina, silica and lime) are put to furnace and melted using EAF technology [29]. They are raw metallurgical slags and have heterogeneous structure [29, 33, 35]. Blast furnace slags (BFA) is formed during steel making process and mainly composed of Akermanite $Ca_2Mg(Si_2O_7)$ with calcium silicate phases (larnite and pseudowollastonite) in low content [29]. Induction furnace slags (IFS) are waste materials generated from melting ferrous metal scraps and fluxes in induction furnaces [36]. Most of these slags such as BOF, EAF slag1, EAF slag2, C EAF Slag (Figure 3 a), S EAF slag and IFS (Figure 3 b) can be used directly without applying any additional processes.

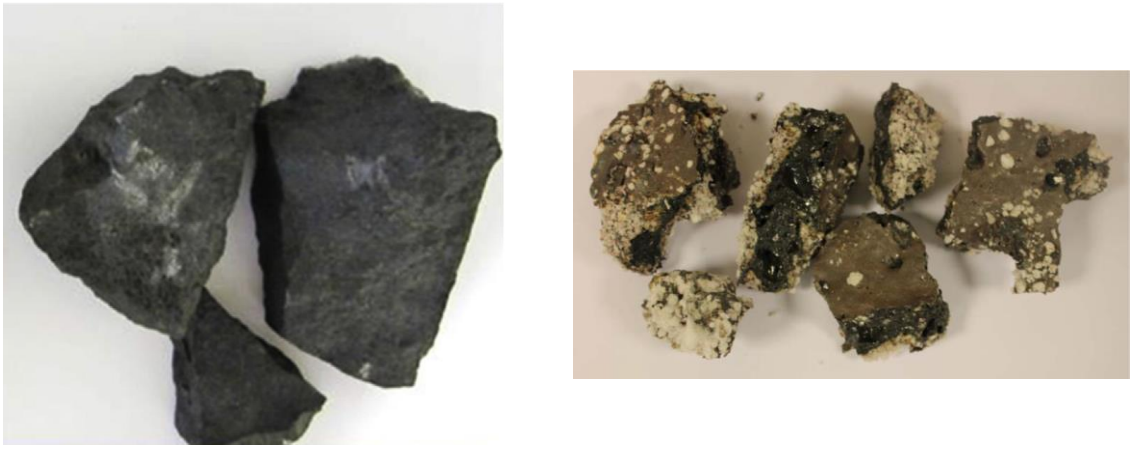

(a) (b)

Figure 3. Industrial by-products; a) EAF Slag [35], b) IFS [36]

Salt-based solid by-products coming from potash industry are also investigated as candidate STESMs. Such wastes can be used directly (Salt A) or after water treatment and molding (Salt B). Basic oxygen furnace (BOF) slag is a by-product from steel industry and it is formed during the solidification of the steel in a basic oxygen furnace [34]. Figure 4 shows these salt-based industrial by-products.

(a) (c)

(b)

Figure 4. Salt-based industrial by-products: a) BOF Slag [34], b) Salt A [39], c) Salt B [39]

3.1.3 Porosity and Microstructure of the prepared samples

Microscopic images are used to analyze the porosity and morphological properties. The average pore size of DW was determined as 242 Å using BET TriStar 3000. This result shows that DW has very low porosity. The optical microscopie image of DW sample at 10X magnification obtained using Zeiss Axiovert S100 shown in Figure 5 confirms this result.

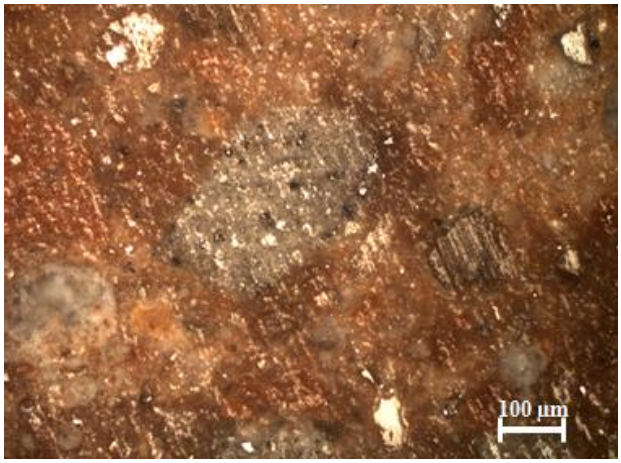

Figure 5. Microscopic image of DW at 10X magnification

Figure 6 shows the Scanning Electron Miscroscope (SEM) images of the cross section of the industrial wastes. Due to the high iron content, EAF has heterogeneous structure and small closed porosities. EAF slag1 and EAF slag2 have regions with different compositions. White regions contain iron, dark regions are composed of calcium, silicon and aluminum and the light grey regions are composed of silicon and calcium [35]. SEM images of C EAF slag (from a steel producer in China) and S EAF slag (from a steel producer in Spain) proves that slags may have some small or coarse pores because of cooling process of liquid steel slag in air. CFA seems very dense with homogeneous structure. There are few small cracks and closed porosities in CFA. BFA (industrial grade ceramic) has some open porosity (black areas) but no micro cracks were observed [29]. This behavior is the same as converter samples. IFS have some white and dark grey regions, which show metallic particles such as iron and oxides like SiO_2, Al_2O_3.

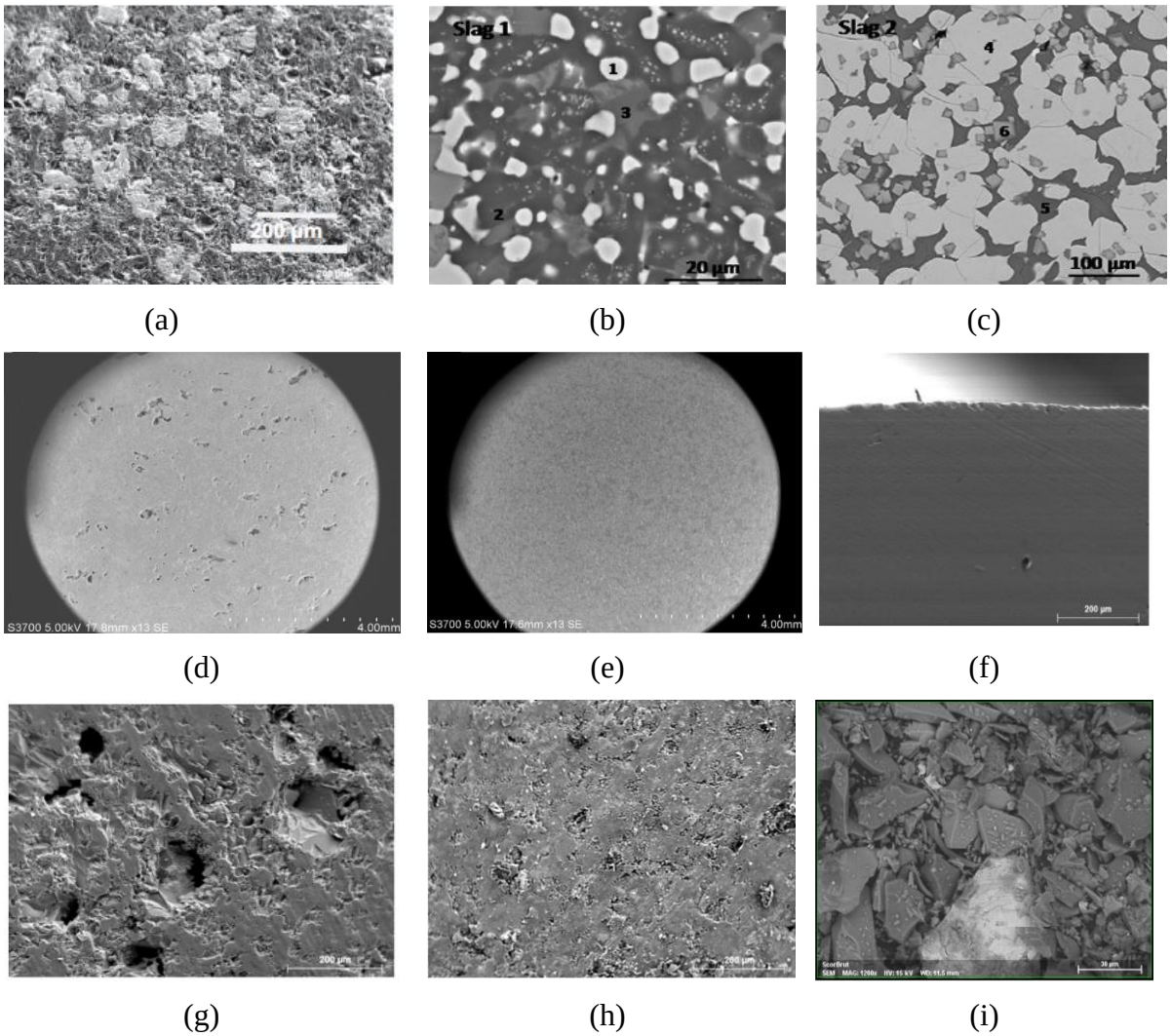

Figure 6. SEM images of industrial wastes a) EAF [29], b) EAF Slag 1 [35], c) EAF Slag 2 [35], d) C EAF Slag [33], e) S EAF Slag [33], f) CFA [29], g) BFA [29], h) Conv [29], i) IFS [36]

Figure 7 shows the ESEM images of the cut of Cofalit samples: (a) plasma torch treated ceramic Cofalit, (b) glassy ceramic by vitrification process. Dark grey regions show Wollastonite with

iron content and light grey regions show Augite. As seen in Figure 7, Cofalit has some closed porosities and micro cracks (black lines).

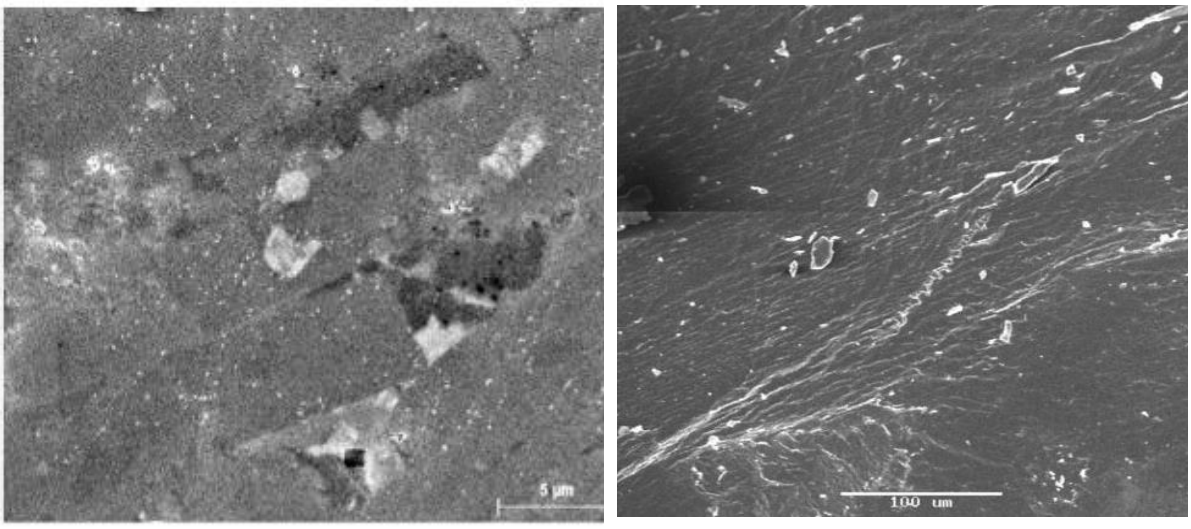

(a) (b)

Figure 7. ESEM images of asbestos containing wastes; (a) ceramic Cofalit by plasma torch treatment [29], (b) Glassy Cofalit by vitrification process [37]

SEM image given in Figure 8 shows multiphase structure of BOF slags. It includes magnesioferrite, larnite, grossular and bixbyite. This structure causes large volume of pores in the material [34].

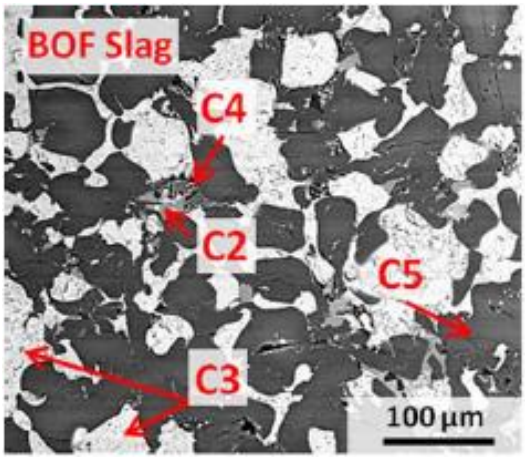

Figure 8. SEM images of BOF [34]

3.2. Mechanical Properties

Crushed storage materials may cause clogging of the storage system and damage pump and other system components. Therefore, storage materials with good mechanical properties are preferred to provide regular flow and durable storage systems [5]. There are few studies on mechanical compressive strength of STESMs. Table 2 shows mechanical strength results of

DW, IB, CBPC-B, CBPC-P, AB, AP, PP and PB. The parameters such as mortar formulation content, molding, humidity, porosity affect the mechanical strength [5].

The compressive strength of the cubic DW samples was measured by single axial load measurement device. Results show that the strength of the DW samples is 5.4 MPa. Compared with IB, DW has higher compressive strength. IB sample was prepared by only compression method without adding additives and its strength was 1.6 MPa. Lower strength value for IB may be caused from its preparation method and high porosity. Mortar formulations prepared from Slag A and Slag P were poured into molds with dimension of 40x40x160 mm^3 to evaluate their mechanical strengths. Their compressive strengths are better than DW and IB samples. Method used in determining the mechanical strength may affect the results.

Table 2. Compressive strength of materials

Sample Name	Compressive Strength, MPa	Ref
DW	5.4	[28]
IB	1.6	[32]
CBPC_B	26.8	[32]
CBPC_P	28.9	[32]
AB	50.7	[32]
AP	42.9	[32]
PP	46.6	[32]
PB	62.6	[32]

3.3. Chemical Properties

Chemical compositions of waste/by-product materials are shown in Table 3. XRF results show that DW is mainly composed of CaO (57.4 %), SiO_2 (17.5%) and Fe_2O_3 (11.6%). Silicon oxide content in storage material is a characteristic property to define material's strength and hardness. Higher amount of silicon oxide avoids crushing during thermal cycling under repeated thermo-mechanical stress [43].

Industrial wastes are mainly composed of silicon oxide (SiO_2), lime (CaO), alumina (Al_2O_3), iron oxides (Fe_2O_3), and magnesia (MgO) [36]. Compared with DW, EAF and BOF slags have higher amount of Fe_2O_3 (>20%). This may cause corrosion reaction with solar salts [29, 34]. EAF slag 1 and 2 are also from steel making process, but their furnace technologies and fluxes (e.g alumina, dolomite, lime) are different.

IFS is mainly composed of Si, Al and Mn, which are related to steel production process. Cofalit has two main phases such as Wollastonite ($CaSiO_3$) and Augite ($(Ca, Mg, Al, Fe)(SiO_3)_2$). It is mainly composed of CaO (17%) and SiO_2 (16%) [29].

WrutF, IB, WDF, BOF and pyrometallurgical slags (Slag P and Slag B) are by-products derived from mining and metallurgical industry. By-products of the pyrometallurgical refining process of copper (Slag P and Slag B) and by-product in electric arc furnace of the steel making process (WDF) are mainly metal oxides. IB is a chloride salt by-product of the potash production and it is generally composed of sodium chloride. WrutF is a derivative from ilmenite mining that contains mostly silica oxide [32].

Table 3. Chemical composition of waste materials.

Composition, %	Ca	Si	Fe	Al	Mg	Mn	Ti	Ref.
DW	57.4	17.5	11.6	2.8	1.2		-	[28]
Cofalit	17.0	16.0	10.0	2	11	0	-	[29]
CFA	13	20	5	8	2	0	-	[29]
EAF	27	10	23	6	1	2	-	[29]
BFA	34	15	0	5	3	0	-	[29]
Conv.	39	4	6	1	1	1	-	[29]
BOF	30.5	14.8	37.3	1.9	4.7	4.8	-	[34]
EAF Slag1	28.5	19.1	24.2	13.4	3.8	0.5	2.1	[35]
EAF Slag2	16.5	11.4	52.3	3.2	4.7	4.4	1.4	[35]
IFS	1.0	24.6	9.7	10.3	0.5	12.8	0.5	[36]

Figure 9 compares FTIR analysis of DW and IFS samples. According to FTIR analysis, IFS has a peak around 1033 cm^{-1}, which is attributed to Si-O band. Close to this band, DW showed a wide peak at around 1008 cm^{-1}. A weak peak at around 2360 cm^{-1}, which shows C-O band was observed in IFS. It proves the absorption of CO_2 during the manipulation of IFS [36]. This peak was not seen in DW. Carbonate minerals such as calcite, aragonite, dolomite and lime can be identified in 1420, 876 and 700 cm^{-1} vibration bands [44]. Peaks in 713, 875 and 1417 confirm that DW is composed of a mixture of carbonates, while silicates are also identified (peak around 1008cm^{-1} corresponding to Si-O vibration). On the other hand, IFS has only a weak peak around 792 cm^{-1}, which shows the small content of quartz [36].

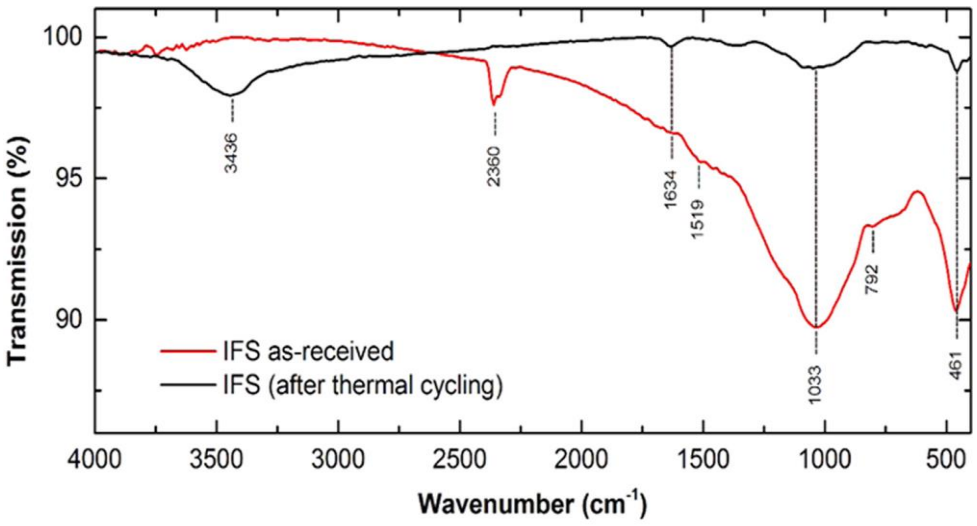

(a)

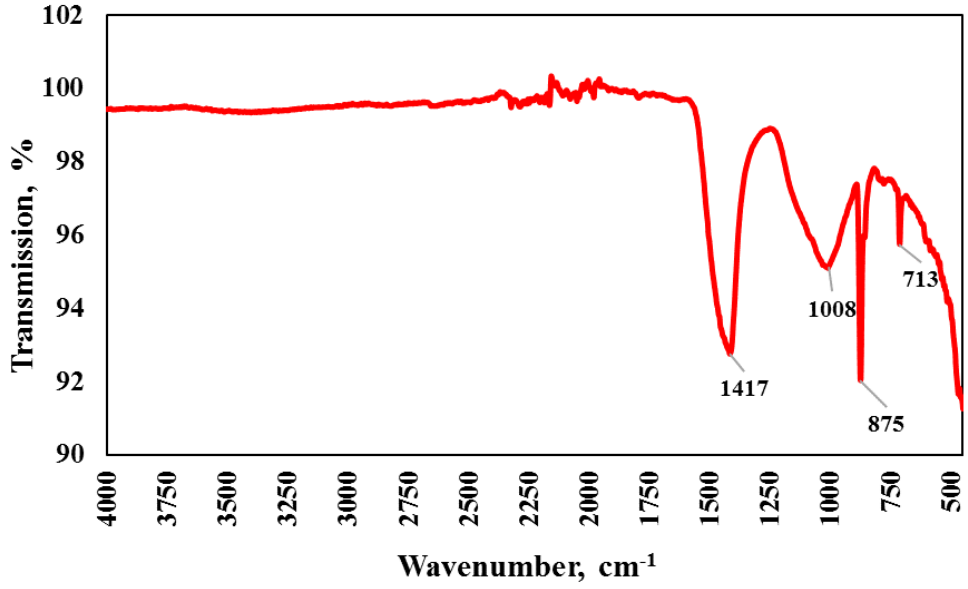

(b)

Figure 9. Infrared Spectroscopy (FTIR) analysis of IFS as received [36] (a) and DW sample (b)

3.4 Thermal Properties

3.4.1 Thermal Conductivity

Thermal conductivity of storage materials is an important parameter to enhance storage performance of TES systems [1]. High thermal conductivity is preferable for STESMs. Thermal conductivities for waste materials are given in Table 4. Thermal conductivity of ceramic Cofalit is 2.1-1.4 $Wm^{-1}K^{-1}$ between 150ºC and 300ºC. Samples with higher iron content have higher thermal conductivity [29]. For example, thermal conductivity of BOF slag having more than 35% iron, reaches up to 2.2 $Wm^{-1}K^{-1}$.

On the other hand, porosity affects thermal conductivity reversely. Air contained within the pores decreases thermal conductivity [32]. Thermal conductivity measurements were

performed in powder form for WrutF, WDF, Slag B, Slag P and Salt A. Therefore, their thermal conductivities are lower than other STESM samples and they need extra processes to increase thermal conductivities. As an example, Miro et al. [39] applied water treatment and molding processes to Salt A to increase its thermal conductivity from 0.33 $Wm^{-1}K^{-1}$ (Salt A) to 2.84 $Wm^{-1}K^{-1}$ (Salt B).

In this study, thermal conductivities of DW both in dust and pellet form were measured. Like other ceramic powder samples, thermal conductivity of DW powder samples was very low (0.10 $Wm^{-1}K^{-1}$). On the other hand, thermal conductivity of DW pellet (0.53$Wm^{-1}K^{-1}$) was higher than the powder form as expected. Although thermal conductivity of DW pellet is higher than powder form, it is lower than the other waste samples from mining industry.

3.4.2 Thermal Stability

DW samples were heated up to 1200°C by TGA. 3.2% mass loss was observed between 100°C to 200°C, mainly from moisture loss. Decomposition started after 750ºC, attributed to carbonates decomposition, which shows DW can be used until this temperature without thermal degradation [28]. Cofalit, CFA and EAF were stable up to 1100ºC [29, 35, 37]. EAF slags were heated up to 1000°C by TGA and mass loss was detected at around 1.3% in the temperature range 100-200ºC, which was related to evaporation of water in the sample.

3.4.3 Storage Capacity

Storage capacity of STESM is strongly dependent on specific heat and density of materials [1]. Specific heat, density and heat capacity of waste samples are summarized in Table 4.

Depending on the material content and porosity, density of industrial wastes can be found at different scales. IFS density is in range of 2036-3413 kgm^{-3}, average density is 2583 kgm^{-3}. EAF slags are in the range of 3430-4260 kgm^{-3}. Densities of BFA and CFA are 2800 and 2600 kgm^{-3}, respectively. The densities of WDF and IB were obtained as 3967 kgm^{-3} and 2100 kgm^{-3}, respectively. Both ceramic and glassy Cofalits have a high density in the range of 3100-3200 kgm^{-3}. WrutF's density is 4154 kgm^{-3} and higher than the other industrial by-products.

The average density of DW dust was measured as 2730 kgm^{-3}. DW has nearly the same density as IFS, BFA, CFA and IB. WDF, EAF slag, Cofalit, Slag P, Slag B and WrutF have higher densities compared to DW. Although their densities are higher than DW, only WrutF has higher specific heat capacity from DW.

The specific heat capacity of ceramic Cofalit is 800-1034 $Jkg^{-1}K^{-1}$ [26, 29]. At 100ºC, the specific heat capacity of WrutF is 749 $Jkg^{-1}K^{-1}$ and it increases to 1085 $Jkg^{-1}K^{-1}$ at 500 ºC. As seen in Table 4, specific heat capacities of EAF slags are in 713 – 933 $Jkg^{-1}K^{-1}$, while for IFS the value of specific heat capacity is between 694-738 $Jkg^{-1}K^{-1}$ in the same temperature range. Average specific heat capacity of DW was determined as 1282 $Jkg^{-1}K^{-1}$ (50-100°C) and 1457 $Jkg^{-1}K^{-1}$ (100-400°C) [28]. Specific heat capacity of DW increases with temperature. The same behavior is observed in other industrial by-products and wastes.

Figure 10 produced by Minitab 18 program in this study compares specific heat capacities of waste materials versus densities. DW has the highest specific heat capacity after WrutF. Density of DW is lower than WrutF and EAF slags.

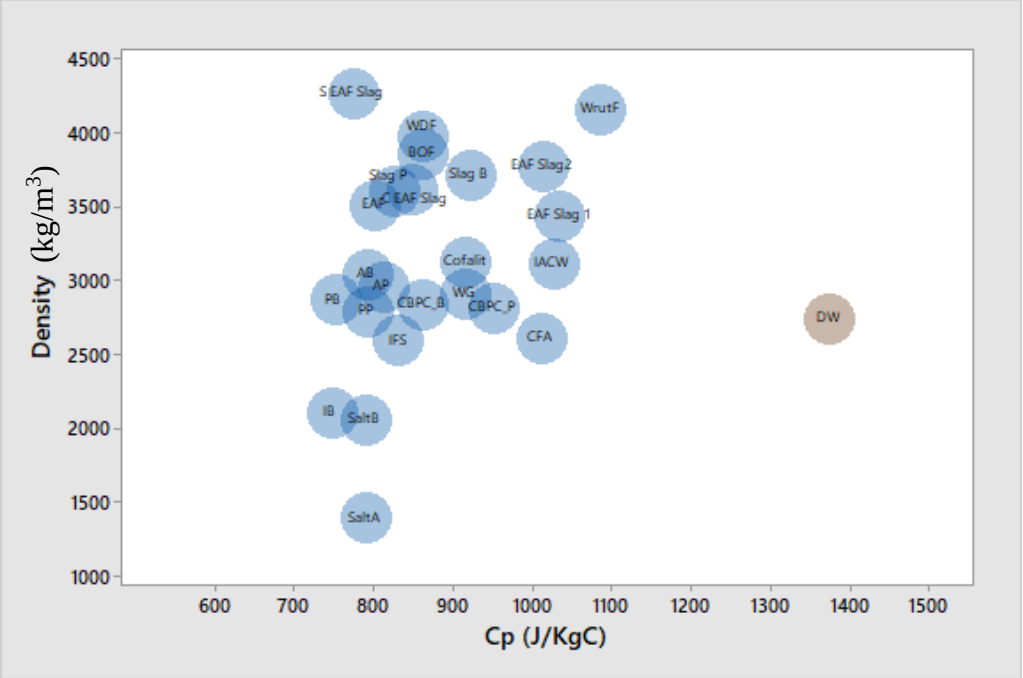

Figure 10. Comparison of properties of DW with other waste materials

3.5 Cost

Waste materials are the main motivation to found cheap STESM with their thermally stable, non-toxic and good storage properties. DW and other waste materials in literature can be suitable for high temperature STES applications. Unit costs of these materials are compared in Table 4 together with storage capacities. The costs vary between 0.001 to 1.20 €/kg.

Figure 11 is produced by Minitab 18 program in this study to compare cost and storage capacities of waste storage materials. As seen in Figure 11, DW has one of the lowest cost in waste materials with value of 0.001 €/kg. WrutF has higher heat capacity with 0.008 €/kg cost. Commercial Cofalit which is used as underlayer material in building roads is also cheap (0.008 €/kg). On the other hand, when Cofalit is treated by plasma torch, its price increases to 1.2 €/kg.

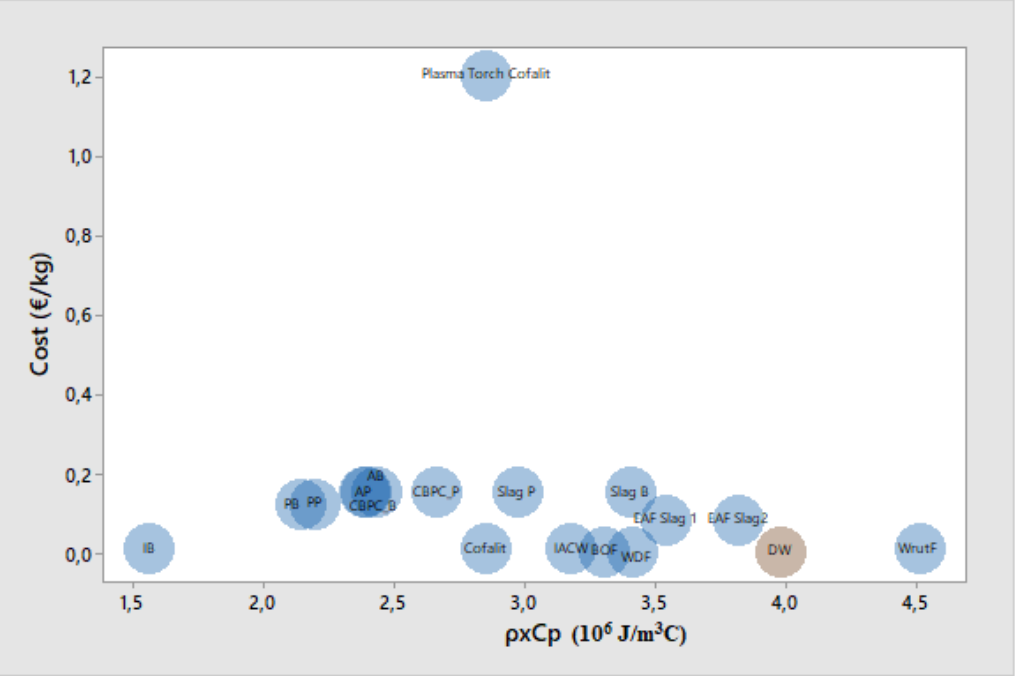

Figure 11. Comparison of properties of DW with other waste materials

Table 4. Properties of STES samples from waste materials.

Material Name	ρ, (kgm^{-3})	C_p, (Jkg^{-1}K^{-1})	ρxC_p, (10^6 Jm^{-3}C^{-1})	Thermal conductivity k, (Wm^{-1}K^{-1})	Cost, €/kg	Ref
DW	2730	1287 $^{(50°C-100°C)}$-1457 $^{(100°C-400°C)}$	3.98	0.1 (powder form) 0.53 (Pellet form)	0.001	[28]
Cofalit	3120	800-1034	2.49-3.22	2.1-1.4	0.008 €/kg [29] 1.20 €/kg (treated by plasma torch) [26]	[26, 29]
IACW	3100	1025	3.18	1.4	0.008 €/kg	[37]
WrutF	4154	749$^{(100°C)}$-1085$^{(500°C)}$	3.1-4.5	0.8	0.008 €/kg	[32]
WDF	3967	855	3.4	0.7	0.001 €/kg	[32]
IB	2100	640-850	1.34-1.78	3-4	0.007 €/kg	[32]
Slag P	3600	571$^{(100°C)}$-1088$^{(500°C)}$	2.05-3.9	0.8	0.15 €/kg	[32]
Slag B	3700	648$^{(100°C)}$-999$^{(500°C)}$	2.40-3.7	1.1	0.15 €/kg	[32]
BOF	3844	750-960	2.74-3.69	1.95-2.2	0€/kg	[27, 34]
SaltA	1384	738	1.02	0.33	NA	[39]
SaltB	2050	738	1,51	2.84	NA	[39]
CBPC_B	2828	703$^{(100°C)}$-1015$^{(500°C)}$	1.99-2.87	1.6	0.15 €/kg	[32]
CBPC_P	2804	655$^{(100°C)}$-1230$^{(500°C)}$	1.84-3.45	1.5	0.15 €/kg	[32]
AB	3030	640$^{(100°C)}$-923$^{(500°C)}$	1.94-2.80	1.4	0.15 €/kg	[32]
AP	2947	630$^{(100°C)}$-985$^{(500°C)}$	1.86-2.90	1.4	0.15 €/kg	[32]
PP	2785	623$^{(100°C)}$-971$^{(500°C)}$	1.74-2.70	1.4	0.12 €/kg	[32]
PB	2859	681$^{(100°C)}$-829$^{(500°C)}$	1.95-2.37	1.8	0.12 €/kg	[32]
IFS	2583 (2036-3413)	694-738	1.79-1.90	NA	NA	[36]
EAF	3500	700	2.45	1.5-2.0	NA	[29]
EAF Slag1	3430	0.933$^{(500°C)}$	3.2	1.43	0.08€/kg	[35]
EAF Slag2	3770	0.912$^{(500°C)}$	3.43	1.41	0.08€/kg	[35]
C EAF Slag	3610	0.717$^{(24°C)}$-0.975$^{(500°C)}$	2.59-3.52	1.75-1.84	NA	[33]
S EAF Slag	4260	0.713$^{(24°C)}$-0.858$^{(500°C)}$	3.04-3.65	1.69-1.74	NA	[33]
BFA	2800	-	-	1-1.5	NA	[29]
CFA	2600	735-1300	1.91-3.38	1.3-2.1	NA	[29]
WG	2900	714-1122	2.1-3.2	1.16-1.59	NA	[23]

4. Conclusions

Valorization of waste material is a sustainable way of creating cost effective TES systems. In this study, DW taken from an urban regeneration project in Adana, Turkey was assessed as STESM and benchmarked with other waste materials as STESM found in literature.

Most of the waste materials should be re-processed by crushing, adding additives, molding, drying etc, to obtain homogeneous samples. Furnace slags can be used directly if regular shape is not needed. Depending on the treatment method, extra process may increase the unit cost of waste material like Cofalit treated by plasma torch (1200 €/kg). The unit cost of STESM from DW is only 0.001 €/kg, the lowest among the other waste STESMs in this study.

The results show that DW was mainly composed of CaO (57.3%), SiO_2 (17.5%) and Fe_2O_3 (11.6%). High amount of silicon dioxide comes from glass materials and increases specific heat capacity of DW.

DW has lower porosity than EAF slags, IB, BOF and BFA. Porosity is an important property affecting the compressive strength of material. The compressive strength of DW (5.4 MPa) is higher than IB, which was prepared by compressive method.

As seen in the results, average specific heat of STESM vary between 1000 – 1460 $Jkg^{-1}C^{-1}$ in temperature range of 100-500 °C and heat capacities vary from 1.0 $.10^6$ $Jm^{-3}C^{-1}$ to 4.5.10^6 $Jm^{-3}C^{-1}$. Heat capacity of DW is 3.2.$10^6Jm^{-3}C^{-1}$, whereas the highest energy density was for WrutF with value of 4.5x10^6 $Jm^{-3}C^{-1}$ due to its higher density. It can be concluded that DW has better storage performance than other waste materials in literature except for WrutF. While the other waste materials were durable up to around 1000 ºC, DW sample was durable until 750 °C.

DW is abundantly available and can be recommended for high temperature thermal energy storage (TES) applications in packed beds up to 750ºC.

Acknowledgements

This study was carried out under a co-tutelle agreement between Cukurova University and University of Barcelona. The authors from Cukurova University thanks BAP Project (no:FDK-2018-9602). The research leading to these results is partially funded by the Spanish government RTI2018-093849-B-C32 MCIU/AEI/FEDER, UE. A.I. Fernández would like to thank the Catalan Government for the quality accreditation given to their research groups DIOPMA (2017 SGR 188)

5. References

[1] A. I. Fernández, M. Martínez, M. Segarra, L. F. Cabeza, Selection of materials with potential in thermal energy storage, Solar Energy Materials and Solar Cells, 94 (2010) 1723-1729. https://doi.org/10.1016/j.solmat.2010.05.035

[2] S. Khare, M. Dell'Amico, C. Knight, S. McGarry, Selection of materials for high temperature sensible energy storage, Solar Energy Materials&Solar Cells, 115 (2013) 114–122. https://doi.org/10.1016/j.solmat.2013.03.009

[3] K.G. Allen, T.W. von Backström, D.G. Kröger, Packed rock bed thermal storage in power plants: design considerations, Energy Procedia 49 (2014) 666 – 675. https://doi.org/10.1016/j.egypro.2014.03.072

[4] K.G. Allen, T.W. von Backstro, D.G. Kroger, Rock bed pressure drop and heat transfer: Simple design correlations, Solar Energy 115 (2015) 525–536. https://doi.org/10.1016/j.solener.2015.02.029

[5] V. Becattini, T. Motmans, A. Zappone, C. Madonna, A. Haselbacher, A. Steinfeld, Experimental investigation of the thermal and mechanical stability of rocks for high-temperature thermal-energy storage, Applied Energy 203 (2017) 373–389. https://doi.org/10.1016/j.apenergy.2017.06.025

[6] A. Bruch, J. F. Fourmigue, R. Couturier, S. Molina, Experimental and numerical investigation of stability of packed bed thermal energy storage for CSP power plant, Energy Procedia 49 (2014) 743 – 751. https://doi.org/10.1016/j.egypro.2014.03.080

[7] M. Diago, A. C. Iniesta, T. Delclos, T. Shamim, N. Calvet, Characterization of desert sand for its feasible use as thermal energy storage medium, Energy Procedia 75 (2015) 2113 – 2118. https://doi.org/10.1016/j.egypro.2015.07.333

[8] M. Hänchen, S. Brückner, A. Steinfeld, High-temperature thermal storage using a packed bed of rocks e Heat transfer analysis and experimental validation, Applied Thermal Engineering 31, (2011) 1798-1806. https://doi.org/10.1016/j.applthermaleng.2010.10.034

[9] Y. Jemmal, N. Zari, M. Maaroufi, Thermophysical and chemical analysis of gneiss rock as low cost candidate material for thermal energy storage in concentrated solar power plants. Solar Energy Materials & Solar Cells, 157 (2016) 377–382. https://doi.org/10.1016/j.solmat.2016.06.002

[10] N. Mertens, F. Alobaid, L. Frigge, B. Epple, Dynamic simulation of integrated rock-bed thermocline storage for concentrated solar power, Solar Energy 110 (2014) 830–842. https://doi.org/10.1016/j.solener.2014.10.021

[11] D. Schlipf, P. Schicktanz, H. Maier, G. Schneider, Using sand and other small grained materials as heat storage medium in a packed bed HTTESS, Energy Procedia 69 (2015) 1029 – 1038. https://doi.org/10.1016/j.egypro.2015.03.202

[12] R. Tiskatine, R. Oaddi, R. A. E. Cadi, A. Bazgaou, L. Bouirden, A. Aharoune, A. Ihlal, Suitability and characteristics of rocks for sensible heat storage in CSP plants, Solar Energy Materials and Solar Cells Volume 169 (2017) 245-257. https://doi.org/10.1016/j.solmat.2017.05.033

[13] S.A. Zavattoni, M.C. Barbato, A. Pedretti, G. Zanganeh, A. Steinfeld, High temperature rock-bed TES system suitable for industrial-scale CSP plant – CFD analysis under charge/discharge cyclic conditions, Energy Procedia 46 (2014) 124 – 133. https://doi.org/10.1016/j.egypro.2014.01.165

[14] C. Martin, A. Bonk, M. Braun, C. Odenthal, T. Bauer, Investigation of the long-term stability of quartzite and basalt for a potential use as filler materials for a molten-salt based thermocline storage concept, Solar energy 171 (2018) 827-840. https://doi.org/10.1016/j.solener.2018.06.090

[15] S. Kiwan, Q. R. Soud, 2019. Numerical investigation of sand-basalt heat storage system for beam-down solar concentrators, Case Studies in Thermal Engineering, 13, 100372, https://doi.org/10.1016/j.csite.2018.100372

[16] R. Tiskatine, A. Aharoune, L. Bouirden, A. Ihlal, Identification of suitable storage materials for solar thermal power plant using selection methodology. Applied Thermal Engineering, 117 (2017) 591–608. https://doi.org/10.1016/j.applthermaleng.2017.01.107

[17] X. Py, N. Sadiki, R. Olives, V. Goetz, Q. Falcoz, 2017. Thermal energy storage for CSP (Concentrating Solar Power), EPJ Web of Conferences 148, 00014. https://doi.org/10.1051/epjconf/20171480

[18] G. Zanganeh, A. Pedretti, S. Zavattoni, M. Barbato, A. Steinfeld, Packed-bed thermal storage for concentrated solar power - Pilot-scale demonstration and industrial- scale design, Sol. Energy 86 (2012) 3084–3098. https://doi.org/10.1016/j.solener.2012.07.019

[19] M. M.S. Al-Azawii, C. Theade, M. Danczyk, E. Johnson, R. Anderson, Experimental study on the cyclic behavior of thermal energy storage in an air-alumina packed bed, Journal of Energy Storage 18 (2018) 239–249. https://doi.org/10.1016/j.est.2018.05.008

[20] M. Cascetta, G. Cau, P. Puddu, F. Serra, A study of a packed-bed thermal energy storage device: test rig, experimental and numerical results, Energy Procedia 81 (2015) 987 – 994. https://doi.org/10.1016/j.egypro.2015.12.157

[21] S. Molina, D. Haillot, A. Deydier, J. P. Bedecarrats, Material screening and compatibility for thermocline storage systems using thermal oil, Applied Thermal Engineering 146 (2019) 252–259. https://doi.org/10.1016/j.applthermaleng.2018.09.094

[22] A. Dinker, M. Agarwal, G.D. Agarwal, Heat storage materials, geometry and applications: A review, Journal of the Energy Institute, 90 (2017) 1-11. https://doi.org/10.1016/j.joei.2015.10.002

[23] A. Gutierrez, A. Gil, J. Aseguinolaza, C. Barreneche, N. Calvet, X. Py, A. I. Fernandez, M. Grágeda, S. Ushak, L. F. Cabeza, Advances in the valorization of waste and by-product materials as thermal energy storage (TES) materials, Renewable and Sustainable Energy Reviews, 59 (2016) 763-783. https://doi.org/10.1016/j.rser.2015.12.071

[24] I. Ortega, A. Faik, A. Gil, J. R. Aseguinolaza, B. D'Aguanno, Thermo-physical properties of a steel-making by-product to be used as thermal energy storage material in a packed-bed system, Energy Procedia 69 (2015) 968 – 977. https://doi.org/10.1016/j.egypro.2015.03.180

[25] I. O. Fernández, Y. Grosu, A. Ocio, P. L. Arias, J. R. Aseguinolaza, A. Faik, New insights into the corrosion mechanism between molten nitrate salts and ceramic materials for packed bed thermocline systems: A case study for steel slag and Solar salt, Solar Energy 173 (2018) 152–159. https://doi.org/10.1016/j.solener.2018.07.040

[26] X. Py, N. Calvet, R. Olivès, P. Echegut, C. Bessada, F. Jay, 2009. Thermal storage for solar power plants based on low cost recycled material. Effstock conference proceedings

[27] Y. Grosu, I. O. Fernández, J. M. L. del Amo, A. Faik, Natural and by-product materials for thermocline-based thermal energy storage system at CSP plant: Compatibility with mineral oil and molten nitrate salt, Applied Thermal Engineering, 136 (2018) 657–665. https://doi.org/10.1016/j.applthermaleng.2018.03.034

[28] B. Koçak, H. Paksoy, Using demolition wastes from urban regeneration as sensible thermal energy storage material, Int J Energy Res., 43 (2019) 6454-6460 https://doi.org/10.1002/er.4471

[29] F. Motte, Q. Falcoz, E. Veron, X. Py, Compatibility tests between Solar Salt and thermal storage ceramics from inorganic industrial wastes, Applied Energy 155 (2015) 14–22. https://doi.org/10.1016/j.apenergy.2015.05.074

[30] N. Calvet, J. C. Gomez, A. Faik, V. V. Roddatis, A. Meffre, G. C. Glatzmaier, S. Doppiu, X. Py, Compatibility of a post-industrial ceramic with nitrate molten salts for use as filler

material in a thermocline storage system, Applied Energy 109 (2013) 387–393. https://doi.org/10.1016/j.apenergy.2012.12.078

[31] K.M. Al Naimi, T. Delclos, N. Calvet, Industrial waste produced in the UAE, valuable high-temperature materials for thermal energy storage applications, Energy Procedia 75 (2015) 2087 – 2092. https://doi.org/10.1016/j.egypro.2015.07.320

[32] M.E. Navarro, M. Martı´nez, A. Gil, A.I. Fernandez, L.F. Cabeza, R. Olives, X. Py, Selection and characterization of recycled materials for sensible thermal energy storage, Solar Energy Materials & Solar Cells 107 (2012) 131–135. https://doi.org/10.1016/j.solmat.2012.07.032

[33] Y. Wang, Y. Wang, H. Li, J. Zhou, K. Cen, Thermal properties and friction behaviors of slag as energy storage material in concentrate solar power plants, Solar Energy Materials and Solar Cells 182 (2018) 21–29. https://doi.org/10.1016/j.solmat.2018.03.020

[34] Y. Grosu, I. Fernández, L. Fernández, U. Nithiyanantham, Y. Baba, A. Mers, A. Faik, Natural and by-product materials for thermocline-based thermal energy storage system at CSP plant: Structural and thermophysical properties, Applied Thermal Engineering, 136 (2018) 185-193. https://doi.org/10.1016/j.applthermaleng.2018.02.087

[35] I. O. Fernandez, N. Calvet, A. Gil, J. R. Aseguinolaza, A. Faik, B. D'Aguanno, Thermophysical characterization of a by-product from the steel industry to be used as a sustainable and low-cost thermal energy storage material, Energy 89 (2015) 601-609. https://doi.org/10.1016/j.energy.2015.05.153

[36] H. Agalit, N. Zari, M. Maaroufi, Thermophysical and chemical characterization of induction furnace slags for high temperature thermal energy storage in solar tower plants, Solar Energy Materials and Solar Cells, 172 (2017) 168–176. https://doi.org/10.1016/j.solmat.2017.07.035

[37] X. Py, N. Calvet, R. Olives, A. Meffre, P. Echegut, C. Bessada, E. Veron, S. Ory, 2011. Recycled material for sensible heat based thermal energy storage to be used in concentrated solar thermal power plants, J. Sol. Energy Eng. 133, 031008, https://doi.org/10.1115/1.4004267

[38] A. Faik, S. Guillot, J. Lambert, E. Ve´ron, S. Ory, C. Bessada, P. Echegut, X. Py, Thermal storage material from inertized wastes: Evolution of structural and radiative properties with temperature, Solar Energy 86 (2012) 139–146. https://doi.org/10.1016/j.solener.2011.09.014

[39] L. Miro, M. E. Navarro, P. Suresh, A. Gil, A. I. Fernández, L. F. Cabeza, Experimental characterization of a solid industrial by-product as material for high temperature sensible thermal energy storage (TES), Applied Energy 113 (2014) 1261–1268. https://doi.org/10.1016/j.apenergy.2013.08.082

[40] A. Attanasio, A. Largo, Valorization of construction and demolition wastes: RE4 building solutions, ProScience 4 (2018) 7-12. https://doi.org/10.14644/amamicam.2017.002

[41] EU Construction & Demolition Waste Management Protocol, September 2016

[42] Waste Framework Directive (2008/98/EC), http://ec.europa.eu/environment/waste/framework/ [Access Date:10.08.2018]

[43] T. Nahhas, X. Py, N. Sadiki, S. Gregoire, Assessment of four main representative flint facies as alternative storage materials for concentrated solar power plants, Journal of Energy Storage 23 (2019) 79–88. https://doi.org/10.1016/j.est.2019.03.005

[44] S. N. Ghosh, 2001. IR Spectroscop, in: V.S. Ramachandran, J. J. Beaudoin (eds), Handbook of analytical techniques in concrete science and technology,William Andrew Inc. 2001, New York, pp:174-204